Modeling reliability data sets with extreme values via *q*-Exponential distribution

Romero Sales Filho, Isis Didier Lins, Márcio das Chagas Moura
Universidade Federal de Pernambuco, Brasil

Enrique López Droguett
University of Maryland, USA

Mehdi Amiri
Technical Data Analysis Inc, USA

1. INTRODUCTION

From the Nonextensive Statistical Mechanics reasoning, several probability distributions, known as *q*-distributions, were developed. Since the Nonextensive Statistical Mechanics assumes interdependencies among the components of a system, these *q*-distributions have the ability of modeling complex systems whose elements present strong interactions [1, 2]. The search for new probabilistic models to describe this kind of systems has substantially increased over the last years [3–5]. The *q*-distributions have been successfully applied to several fields of science and engineering. Among them, we can mention complex systems such as cyclones [6], gravitational systems [7], stock market [8, 9], journal citations [10], complex DNA structural organization [11], reliability analysis [5], cosmic rays [12], earthquakes [13], financial markets [14], internet [15], mechanical stress [16].

Picoli *et al*. [3] described the basic properties of three distributions of this kind: *q*-Exponential, *q*-Gaussian and *q*-Weibull. In another work, Picoli *et al*. [4] presented a comparative study, where the *q*-Exponential, *q*-Weibull, and Weibull distributions were used to investigate frequency distributions of basketball baskets, cyclone victims, brand-name drugs by retail sales and highway length.

In fact, q-Exponential distribution is obtained by maximizing the non-extensive entropy under appropriate constraints[17]. This distribution has two parameters (q and η), differently from the Exponential distribution that is one parametric. This feature gives more flexibility to q-Exponential distribution with regard to its decay for the Probability Density Function (PDF) curve.

A prominent point of the q-Exponential distribution is its ability to model data that presents a power law behavior [4] when the q parameter lie within the interval (1, 2). Thus, in the context of reliability, it is expected that for a given sample with large values (e.g., realizations of rare events), the *q*-Exponential distribution can fit the data well.

The stretched exponential provides a compromise between Exponential and power law behaviors. As pointed out by Laherrère and Sornette [18], a stretched exponential probability density function (PDF) has a tail that is heavier than that of the Exponential PDF but lighter than that of a pure power law PDF. The Weibull distribution, for example, presents a behavior of stretched exponential when its shape parameter lies between 0 and 1.

Another important characteristic of the *q*-Exponential is its ability in model the degradation or the improvement of a system. These features may indicate the *q*-Exponential distribution as an alternative to the Weibull distribution. However, these distributions have different origins: while the *q*-Exponential distribution arises from the nonextensive formalism [19], the physical model that justifies the Weibull distribution stems from the theory of extreme values [20].

2. OBJECTIVES OF THE WORK

The present work focuses on the q-Exponential MLE. It is worth mentioning that, in order to obtain analytical expressions for estimators of q-Exponential parameters, it is necessary to solve a complicated set of equations. In this way, Shalizi [21] and Bercher and Vignat [22] have shown that a reparameterization for that set of equations is required. However, this approach allows obtaining analytical expressions for the MLE only when $1 < q < 2$ and, however, the q-Exponential distribution is also defined for $q < 1$. Such a parameter range corresponds to a hazard rate behavior with relevant applications, namely the reliability modeling of degrading systems. In this way, with the exception of the case $1 < q < 2$ [21], analytical expressions for the maximum likelihood estimators of q-Exponential are very difficult to be obtained due to the intricate derivatives of the log-likelihood function.

Thus, in this work the MLE for the parameters of a q-Exponential distribution are numerically derived through two different optimization algorithms: Nelder-Mead [23] and Particle Swarm Optimization (PSO) [24]. The results obtained from these two approaches will be compared by means of bias and MSE (Mean Squared Error). An application example in the context of fatigue life data is developed.

3. THE q-EXPONENTIAL DISTRIBUTION

The following expression represents the q-Exponential PDF:

$$f_q(t) = \frac{(2-q)}{\eta} \exp_q \left[-\left(\frac{t}{\eta}\right)\right], \tag{1}$$

for $q < 2$ and $\eta > 0$. The shape of the distribution is determined by the parameter q, η is the scale parameter and $\exp_q(x)$ is the q-Exponential function defined as:

$$\exp_q(x) = \begin{cases} [1+(1-q)x]^{\frac{1}{1-q}}, & if\ [1+(1-q)x] \geq 0 \\ 0, & \text{otherwise}, \end{cases} \tag{2}$$

where x and $q \in \mathbb{R}$. From the definition of q-Exponential function, it is possible to rewrite the density of the q-Exponential distribution as:

$$f_q(t) = \frac{(2-q)\left[1-\frac{(1-q)t}{\eta}\right]^{\frac{1}{1-q}}}{\eta}, \tag{3}$$

for $q < 2$ and $\eta > 0$. According to the parameter q, the support t is changed as follows:

$$t \in \begin{cases} [0;\ \infty), & q \geq 1. \\ \left[0; \frac{1}{\frac{1}{\eta}(1-q)}\right), & q < 1. \end{cases} \tag{4}$$

As it can be observed in the PDF of the q-Exponential, there are two parameters (q and η), differently from the Exponential distribution that has just one parameter (η). This feature gives more flexibility to the q-Exponential distribution with regard to its decay. Note that, the q-Exponential distribution is a generalization of the Exponential distribution. This fact can be verified when its parameter q tends to one.

Observe yet that for the q-Exponential distribution, the q parameter together with the parameter η determine the decay of the PDF curve. In fact, for a fixed η, the q-Exponential presents a slower decay for $1 < q < 2$ (Power Law characteristic) and a faster decay for $q < 1$; for a fixed q, we have a similar behavior of the Exponential distribution ($q \rightarrow 1$), i.e., as the value of the parameter η increases it is observed a slower decay of the PDF. Figure 1Figure 2 present the q-Exponential PDF for some possible values of q and η.

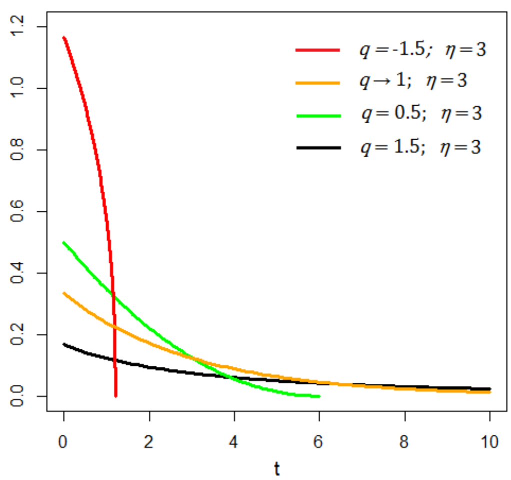

Figure 1 - Behavior of the q-Exponential PDF for a fixed parameter η.

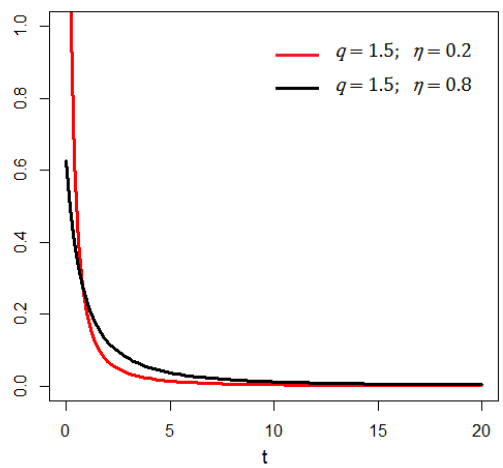

Figure 2 - Behavior of the q-Exponential PDF for a fixed parameter $\boldsymbol{q}$.

The cumulative distribution function (CDF) of the q-Exponential is defined by the following expression:

$$F_q(t) = \begin{cases} 1 - \left[1 - \frac{(1-q)t}{\eta}\right]^{\frac{2-q}{1-q}} t \geq 0, \\ 0, \ \text{otherwise}. \end{cases} \tag{5}$$

A q-Exponential random number generator can be obtained inverting $F_q(t)$ as follows:

$$T = \frac{\eta\left[1-(U)^{\frac{1-q}{2-q}}\right]}{1-q}, \tag{6}$$

where U is a uniform random variable defined in $[0,1]$.

An important characteristic of the q-Exponential distribution, especially in the reliability context, is that the q-Exponential hazard rate function is not necessarily constant as occurs for the Exponential distribution. In fact, we can model two additional behaviors for the hazard rate. Let us first define the hazard rate:

$$h_q(t) = \frac{f_q(t)}{R_q(t)} = \frac{\frac{(2-q)\left[1-\frac{(1-q)t}{\eta}\right]^{\frac{1}{1-q}}}{\eta}}{\left[1-\frac{(1-q)t}{\eta}\right]^{\frac{2-q}{1-q}}} = \frac{(2-q)}{\eta}\left[1-\frac{(1-q)t}{\eta}\right]^{\frac{q-1}{1-q}} \tag{7}$$

Thus, the q-Exponential distribution is able to represent three different types of hazard rate behaviors depending on the values the parameter q. For $1 < q < 2$, $h_q(t)$ is a decreasing monotonic function (Figure 3), for $q < 1$, $h_q(t)$ increases monotonically (Figure 4), while for $q \rightarrow 1$ we have a constant hazard rate.

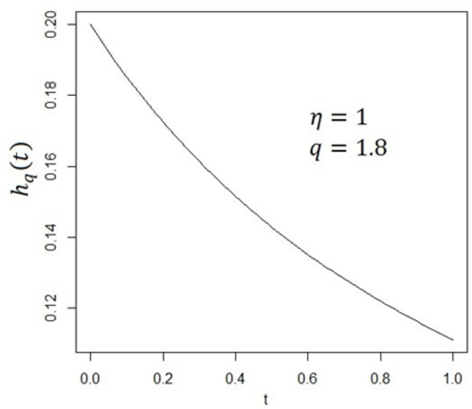

Figure 3 - q-Exponential with decreasing $h_q(t)$

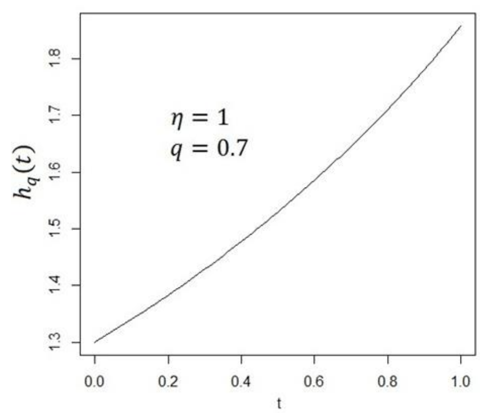

Figure 4 - q-Exponential with increasing $h_q(t)$

4. ESTIMATION OF THE MLE BY OPTIMIZATION METHODS

In order to compute the MLE of q and η let $X = \{x_1, x_2,..., x_n\}$ be a random sample of size n. From this sample, it is possible to write the likelihood function for the observed sample as:

$$L(x,q,\eta) = (2-q)^n \left(\frac{1}{\eta}\right)^n \prod_{i=1}^{n}\left[1-\frac{(1-q)x_i}{\eta}\right]^{\frac{1}{1-q}} \tag{8}$$

and the log-likelihood function as:

$$\mathcal{L}(x,y,r,\beta,q,\eta) = n\,ln(2-q) + n\,ln\left(\frac{1}{\eta}\right) + \frac{1}{1-q}\sum_{i=1}^{n} ln\left[1-\frac{(1-q)x_i}{\eta}\right]. \tag{9}$$

Thus, using an algorithm to maximize the log-likelihood function, we can obtain the estimates for the parameters q and η. In this work, we will call these estimates as $\hat{q}$ and $\hat{\eta}$, and they will be obtained by PSO and Nelder-Mead algorithm, which are described in Sections 4.1 and 4.2, respectively.

4.1 Particle Swarm Optimization

PSO [24] is a probabilistic optimization heuristic based on the motion of groups of organisms (e.g., flocks of birds, schools of fishes), which optimizes a problem from a population of candidate solutions (particles). According to update equations over the particles' position and velocities, the candidate solutions explore the search-space. Each particle's movement is influenced by its own best position and also by its neighbors' best. Thus, it is expected that particles move toward the best solutions. PSO has been successfully applied to different contexts. For example, [24–31] apply PSO in the adjustment of the hyperparameters that emerge in the training problem of support vector machines (SVM). Indeed, Lin et al. [25] , Lins et al. [32] and Droguett et al. [31] use PSO not only to adjust the SVM hyperparameters, but also for variable selection. In the specific context of parameter estimation, PSO has been used to estimate the parameters of a generalized renewal process in order to establish preventive maintenance policies [33], to estimate parameters of mathematical models related to chemical processes [34] and to obtain maximum likelihood estimates for the parameters of a mixture of two Weibull distributions [35].

For a particle j, j = 1, ..., n_{part} , we have the following features:

- Current position in the search space (s_j);
- Best position it has visited so far (p_j);
- Velocity (v_j);
- Fitness (f_j), which is the value of the objective function, which in this work is the q-Exponential log-likelihood ($\mathcal{L}(x, y, r, \beta, q, \eta) = n\, ln(2-q) + n\, ln\left(\frac{1}{\eta}\right) + \frac{1}{1-q}\sum_{i=1}^{n} ln\left[1 - \frac{(1-q)x_i}{\eta}\right]$. (9).

Every particle is a potential solution for the considered optimization problem, which involves a d-dimensional search space with each dimension related to one of the decision variables. Thus, s_j, p_j and v_j are all d-dimensional vectors, whose entries are associated with the decision variables of the problem. In the maximum likelihood optimization problem related to the q-Weibull distribution, d= 2 and the first and second entries of s_j, p_j and v_j are related to η and q, respectively.

The velocity and position update equations are defined as follows:

$$v_{jk}(r+1) = \chi\{v_{jk}(r) + c_1u_1[p_{jk}(r) - s_{jk}(r)] + c_2u_2[p_{gk}(r) - s_{jk}(r)]\}, \tag{10}$$
$$s_{jk}(r+1) = s_{jk}(r) + v_{jk}(r+1), \tag{11}$$

where r is the iteration number, χ is the constriction factor that avoid velocity explosion during PSO iterations [35], c_1 and c_2 are positive constants, u_1 and u_2 are independent uniform random numbers in [0, 1], and p_{gk} is the k-th entry of vector p_g related to the best position that has been found by any neighbor of particle j.

Whenever an infeasible particle emerges - with respect to the constraints over η and q to assure the probabilistic characteristics of the q-Exponential distribution as well as to the logarithm arguments in Eq. 09 - its velocity and its position are not altered and its fitness is not evaluated so as to avoid infeasible p_j and p_g. In this way, infeasible particles may become feasible in subsequent iterations due to the influence of their own and neighbor's feasible best positions. This approach is known as "let particles fly" [24].

The update of velocities and positions and fitness evaluations are repeated until one of the following stop criteria is met:

a) Maximum number of iterations (n_{iter}).

b) The global best particle is the same for 10% of n_{iter}. In this case, the iteration number in which the best particle has been found is used, as commented in the previous subsection.

c) The global best fitness values in two consecutive iterations are different, but such a difference is less than a predefined tolerance δ.

4.2 Nelder–Mead

The Nelder–Mead method, also known as Downhill Simplex Method, is a numerical approach commonly applied to nonlinear optimization problems for which derivatives may not be known. It is used to find the minimum or maximum of an objective function in a multi-dimensional space. This method has been used in several studies with the aim of maximizing the log-likelihood function and to estimate the parameters of various probability distributions in many areas such as: Ecology [37], Medicine [36, 37], Power Systems [38, 39] and Chemical Engineering [42].

This method has been one of the direct search methods most used in unconstrained optimization problem of a function of n variables. The following characteristics make it one of the most popular methods of optimization [43]:

- Ease of computational implementation;
- Calculations of the derivatives of the objective function are not required;
- Few evaluations of the objective function are required;
- The value of the objective function sharply decreases in the first iterations.

The method uses the concept of a simplex, which is a polytope with $n+1$ vertices in n dimensions.

Consider the problem of unconstrained minimization:

$$\min_{x \in \Re^n} \; f(x); \text{ Where, } f: \Re^n \longrightarrow \Re.$$

In one iteration of the Nelder-Mead method, the $n + 1$ vertices of the simplex, $x_1, x_2, \dots, x_{n+1}$ belonging to $\Re^n$ are ordered according to the growth of the values of f, i.e: $f(x_1) \leq f(x_2) \leq \dots \leq f(x_{n+1})$, where x_1 is the best vertex and x_{n+1} is the worst vertex.

The repositioning of these vertices takes into consideration four coefficients:

- Reflection coefficient (ρ)
- Expansion coefficient (χ)
- Contraction coefficient (γ)
- Reduction coefficient (σ)

These coefficients must satisfy the following restrictions[23]: $\rho > 0$, $\chi > 1$, $0 < \gamma < 1$ and $0 < \sigma < 1$. The default choice of these coefficients is given by: $\rho = 1$, $\chi = 2$, $\gamma = 1/2$ and $\sigma = 1/2$

The method attempts to replace the worst vertex of the simplex by one with better value. The new vertex is obtained by reflecting, expansion or contraction of the worst vertex along the line through this vertex and the centroid of the best n vertices. At each iteration, the worst vertex is replaced by a new vertex or the simplex is reduced around the better vertex.

The following steps correspond to an interaction of the Nelder-Mead algorithm[43]:

Step 1 - Sort: Sort the $n+1$ vertices: $f(x_1) \leq f(x_2) \leq \dots \leq f(x_{n+1})$;

Step 2- Centroid: Calculate the centroid of the n best vertices: $\bar{x} = \sum_{i=1}^{n} \frac{x_i}{n}$

Step 3- Reflected vertex: Calculate the reflected vertex (x_r): $x_r = \bar{x} + \rho(\bar{x} - x_{n+1})$

If $f(x_1) \leq f(x_r) \leq f(x_n)$, then do $x_{n+1} = x_r$ and finalize the iteration.

Step 4- Expansion: If $f(x_{\mathrm{r}}) \leq f(x_1)$, calculate the expanded vertex (x_e): $x_e = \bar{x} + \chi(x_r - \bar{x})$
If $f(x_e) \leq f(x_{\mathrm{r}})$, then do $x_{n+1} = x_e$ and finalize the iteration, else $x_{n+1} = x_r$ and finalize the iteration.

Step 5- Contraction: If $f(x_{\mathrm{r}}) \geq f(x_{\mathrm{n}})$

5.1 External: If $\mathrm{f}(\mathrm{x_n}) \leq \mathrm{f}(\mathrm{x_r}) \leq \mathrm{f}(\mathrm{x_{n+1}})$, calculate the external contraction vertex (x_{ce}): $x_{ce} = \bar{x} + \gamma(x_r - \bar{x})$
If $f(x_{ce}) \leq f(x_{\mathrm{r}})$, then do $x_{n+1} = x_{ce}$ and finalize the iteration, else go to step 6.

5.2 Internal: If $f(x_r) \geq f(x_{\mathrm{n+1}})$, calculate the internal contraction vertex (x_{ci}):$x_{ci} = \bar{x} - \gamma(\bar{x} - x_{n+1})$
If $f(x_{ci}) \leq f(x_{\mathrm{n+1}})$, then do $x_{n+1} = x_{ci}$ and finalize the iteration, else go to step 6.

Step 6- Reduction: Calculate de vectors $v_i = x_1 + \sigma(x_i - x_1)$, $i = 2, \ldots, n+1$.
The vertices (not ordered), for the next iteration are: $x_1, v_2, \ldots, v_{n+1}$.

Given a tolerance Δ_{tol}, the following stop criterion [23] takes into account the function value in the simplex vertices: $\sqrt{\sum_{i=1}^{n+1} \frac{\left(f(x_i) - f(\bar{x})\right)^2}{n}} < \Delta_{tol}$

5. NUMERICAL EXPERIMENTS

In this section, some simulations will be presented in order to assess the quality of estimates obtained from PSO and Nelder-Mead methods. We will consider sample sizes equal to 100, 500 and 1000. For the analysis of the MLE we consider the following sets of initial parameters: (η, q) = (5, 1.5), (5, 1), (5, 0.5), and (5, -1). These sets are chosen in order to consider the four important situations for the parameter q: $1 < q < 2$; $q \to 1$; $0 < q < 1$ and $q < 0$. For each set of parameters we generate, by Eq. 06, 1000 samples. Thus, for each one of these samples, we obtained estimates for q and η by PSO and Nelder-Mead algorithms, which resulted in a total of 1000 estimates for each parameter. Table 1 presents the mean of these 1000 estimates for each parameter ($\hat{\eta}$ and $\hat{q}$). Moreover, we reported in Table 1 the related bias and MSE. For an estimator $\hat{\theta}$ of θ, we have that bias$(\hat{\theta}) = E(\hat{\theta}) - \theta$ and MSE $= Var(\hat{\theta}) + bias(\hat{\theta})^2$.

Table 1 - Simulation results for 1000 replications

		PSO						Nelder-Mead					
(η, q)	n	$\hat{\eta}$	$\hat{q}$	Bias $(\hat{\eta})$	Bias $(\hat{q})$	MSE $(\hat{\eta})$	MSE $(\hat{q})$	$\hat{\eta}$	$\hat{q}$	Bias $(\hat{\eta})$	Bias $(\hat{q})$	MSE $(\hat{\eta})$	MSE $(\hat{q})$
(5, 1.5)	100	5.3316	1.4879	0.3316	-0.0121	2.1541	0.0029	5.3317	1.4879	0.3317	-0.0121	2.1550	0.0029
	500	5.0713	1.4982	0.0713	-0.0018	0.3700	0.0005	5.0713	1.4982	0.0713	-0.0018	0.3702	0.0005
	1000	5.0432	1.4983	0.0432	-0.0017	0.1743	0.0003	5.0432	1.4983	0.0432	-0.0017	0.1743	0.0003
(5, 1)	100	5.4545	0.9546	0.4545	-0.0454	2.2459	0.0199	5.4624	0.9540	0.4624	-0.0460	2.3019	0.0204
	500	5.1078	0.9886	0.1078	-0.0114	0.3042	0.0025	5.1175	0.9880	0.1175	-0.0120	0.3614	0.0027
	1000	5.0566	0.9954	0.0566	-0.0046	0.1424	0.0012	5.0716	0.9945	0.0716	-0.0055	0.2311	0.0015
(5, 0.5)	100	5.7744	0.3627	0.7744	-0.1373	3.4889	0.0952	5.8005	0.3592	0.8005	-0.1408	3.6409	0.0984
	500	5.1240	0.4767	0.1240	-0.0233	0.3339	0.0080	5.1767	0.4708	0.1767	-0.0292	0.6679	0.0119
	1000	5.0731	0.4867	0.0731	-0.0133	0.1444	0.0034	5.1905	0.4738	0.1905	-0.0262	0.8922	0.0119
(5, -1)	100	7.8208	-2.248	2.8208	-1.2482	54.1635	10.064	7.51025	-2.115	2.5103	-1.1153	33.1753	6.1973
	500	5.3779	-1.1686	0.3779	-0.1686	0.9296	0.1657	5.3737	-1.167	0.3737	-0.1668	0.9220	0.1643
	1000	5.1939	-1.0869	0.1939	-0.0869	0.3369	0.0583	5.1913	-1.086	0.1913	-0.0858	0.3342	0.0579

From Table 1, we can observe that the estimates obtained by PSO and Nelder-Mead algorithms present bias and MSE that decrease as the sample size (n) increases, corroborating the consistency of the MLE. Also, PSO presents better performance than Nelder-Mead as the former has smaller values for the bias and MSE for the PSO. Despite this, it is important to mention that, in most of the cases, the difference between the bias and MSE obtained from the two algorithms is very small. Also note that identical results were obtained from both algorithms for the MLE estimates, bias and MSE in the case of $\eta = 5$ and $q = 1.5$. Another important point is that when we deal with the case $(\eta, q) = (5, -1)$ and $n = 100$, the PSO and Nelder-Mead method present high values for bias and MSE.

6. APPLICATION EXAMPLE

In this section, we provide estimates of the q-Exponential parameters for fatigue life of high-strength steel that was first reported in [44]. Once this data was obtained from a very resistant material, it is natural that the cycles until failure present great orders of magnitude. Another important point, is that according to Basquin's law, the lifetime of a material increases as a power law [45], and this type of behavior can be modeled by a q-Exponential distribution when $1 < q < 2$.

We will also consider the modeling of data by a Weibull distribution in order to compare the efficiency of these two distributions for this kind of data.

From [44], we get data obtained from a specimen of high-strength steel with diameter 3 mm (Ø3). The data sets given in terms of number of cycles to failure are presented in

Table **2**:

Table 2. Ø3 specimen fatigue test data.

Specimen Number	Fatigue Life (number of cycles to failure)	Specimen Number	Fatigue Life (number of cycles to failure)	Specimen Number	Fatigue Life (number of cycles to failure)
1	1017286	**7**	13007977	**13**	376711232
2	2989152	**8**	25303118	**14**	731957760
3	4059346	**9**	33621704	**15**	9444513800
4	4256299	**10**	55951560	**16**	9912163300
5	8376572	**11**	101155984	**17**	9918688300
6	9560400	**12**	144322192	**18**	9921105900

For this example we will use PSO and Nelder-Mead, in order to obtain the q-Exponential parameters.

The results for the point estimates, when we use PSO approach was: $\hat{\eta} = 4688695.8075$, $\hat{q} = 1.7521$ and the result for the log-likelihood was $\hat{\mathcal{L}} = -374.2125$. The 30 PSO replications essentially provided the same estimates with standard deviations (0.2236, 3.3262E-9 and 5.7800E-14 for η, q and $\mathcal{L}$ estimates, respectively). For the Nelder-Mead approach, the estimated MLE parameters are $\hat{\eta} = 4704629$ and $\hat{q} = 1.7519$, with $\hat{\mathcal{L}} = -374.2075$.

We can observe that both approaches provide similar results. The q estimates lie within (1, 2), which indicates a power law behavior.

Using the Weibull distribution to model the data of this example, we obtain the following results for the parameters: 0.3366 (shape parameter) and 417229710 (scale parameter). For the Weibull distribution, when we have the result of the shape parameter between 0 and 1 it is characterized a behavior of stretched exponential, which in fact is expected for the data of the example, once extremely large values are present. In this example, the parameters' estimates of the Weibull distribution are obtained by analytical expression in the case of the scale parameter and by the Newton-Raphson method for the shape parameter [46].

In order to evaluate the adjustments of this data by a q-Exponential and Weibull distribution, we use the bootstrapped Kolmogorov-Smirnov test (K-S boot). In fact, the one-sample Kolmogorov-Smirnov test (K-S test) is not very useful in practice once it requires that the distribution must be completely specified with all parameters known beforehand [47]. Thus, in this work a bootstrapped version of a K-S test was used as alternative to overcome this problem [48]. This method results in accurate asymptotic approximations of the p-values [49]. Table 3 present the result for the estimated parameters for the q-Exponential and Weibull distributions, together with the results for the K-S boot.

Table 3. Comparing Weibull vs $\boldsymbol{q}$-Exponential.

Parameters (q-Exponential) PSO		**K-S Boot (q-Exponential) PSO**		**Parameters (q-Exponential) Nelder-Mead**		**K-S Boot (q-Exponential) Nelder-Mead**		**Parameters (Weibull)**		**K-S Boot (Weibull)**	
$\hat{\eta}$	$\hat{q}$	**K-S (D_0)**	***p*-value**	$\hat{\eta}$	$\hat{q}$	**K-S (D_0)**	***p*-value**	**Shape Parameter**	**Scale Parameter**	**K-S (D_0)**	***p*-value**
4688695.8075	1.7521	0.1327	0.4860	4704629	1.7519	0.1329	0.4895	0.3366	417229710	0.1648	0.2047

From the results presents in Table 3 we observe that, although the Weibull fit is significant, it is clear that the q-Exponential distribution showed a better fit to the data (either by PSO or Nelder-Mead). Indeed, we observe for this example p-values equal to 0.2047 (for the Weibull distribution), 0.4860 (for the q-Exponential distribution – PSO) and 0.4895 (for the q-Exponential distribution – Nelder-Mead). Clearly the q-Exponential distribution showed a better efficiency, since the data in this example are constituted of extremely large values, with 10^9 as order of magnitude. As mentioned previously, the PDF with power law behavior presents a tail heavier than that of a stretched exponential, thus for data with extremely large values the q-Exponential model is expected to provide a better fit when compared to the adjustment of a Weibull distribution.

Figure 5 present the empirical and theoretical CDFs (Weibull and q-Exponential) for this example. Once the estimates obtained from the two methods (PSO and Nelder-Mead) are very similar, we choose the estimates obtained from the PSO to construct the curves in the graphic. The figure is plotted in logarithmic scale in order to provide a better visualization of the empirical CDF, as the data set contains extremely large values. As we can note from Figure 5, the empirical curve is very close to the q-Exponential CDF, confirming that the q-Exponential model is more efficient than the Weibull distribution when we deal with the type of data presented in this example.

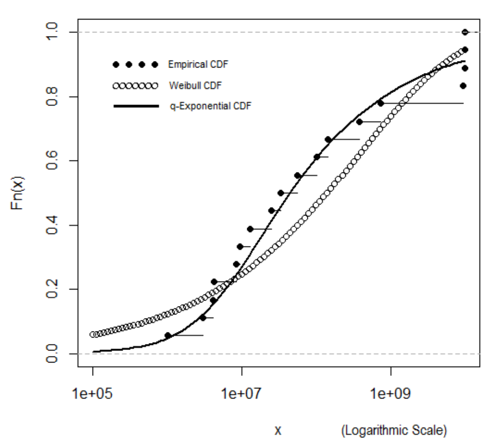

Figure 5 - Empirical and Theoretical (***q***-Exponential and Weibull) CDFs.

7. CONCLUSIONS

In this paper, we have addressed the problem of estimating the q-Exponential parameters by the maximum likelihood method. Once the analytical expression for these parameters are very difficult to be obtained, we use the PSO and Nelder-Mead algorithms in order to maximize the log-likelihood function of the q-Exponential distribution.

From the simulation experiments, it was shown that, for the point estimates, the absolute bias and the MSE values related to the estimation of η and q parameters via maximum likelihood decreases as the sample size increases, indicating the consistency of the MLE. This fact was observed for both algorithms (PSO and Nelder-Mead). Another important particularity of the point estimates is that the PSO algorithm generally presents the lower values for the bias and MSE although the bias and MSE for the Nelder-Mead algorithm were also very good.

For the application example, the Weibull distribution presented significant adjustment, however, the fit by a q-Exponential distribution presented a p-value clearly more significant. Thus, data with extremely large values are well fitted by a q-Exponential distribution, given that this distribution can model the power law behavior when $1 < q < 2$, which is characterized by a PDF with a heavy tail. Therefore, the q-Exponential distribution can be used in several applications of reliability engineering.

8. REFERENCES

[1] A. Der Kiureghian and J. Song, “Multi-scale reliability analysis and updating of complex systems by use of linear programming,” *Reliab. Eng. Syst. Saf.*, vol. 93, no. 2, pp. 288–297, 2008.

[2] P. Bak, *How nature works. The science of self-organized criticality*, 1st ed. Copernicus, 1996.

[3] S. Picoli, R. S. Mendes, L. C. Malacarne, and R. P. B. Santos, “q -distributions in complex systems : a brief review,” *Brazilian J. Phys.*, vol. 39, no. 2A, pp. 468–474, 2009.

[4] S. Picoli, R. S. Mendes, and L. C. Malacarne, “q-exponential, Weibull, and q-Weibull distributions: an empirical analysis,” *Phys. A Stat. Mech. its Appl.*, vol. 324, no. 3–4, pp. 678–688, Jun. 2003.

[5] E. M. Assis, E. P. Borges, and S. A. B. V. De Melo, “Generalized q-Weibull model and the bathtub curve,” *Int. J. Qual. Reliab. Manag.*, vol. 30, no. 7, pp. 720–736, 2013.

[6] a. M. Reynolds and M. Veneziani, “Rotational dynamics of turbulence and Tsallis statistics,” *Phys. Lett. A*, vol. 327, no. 1, pp. 9–14, Jun. 2004.

[7] E. M. C. Abreu, J. A. Neto, and C. F. L. Godinho, “Nonextensive statistics, entropic gravity and gravitational force in a non-integer dimensional space,” *Phys. A Stat. Mech. its Appl.*, vol. 411, pp. 118–127, Oct. 2014.

[8] P. C. Ivanov, A. Yuen, and P. Perakakis, “Impact of stock market structure on intertrade time and price dynamics,” *PLoS One*, vol. 9, no. 4, 2014.

[9] G. Gu, X. Xiong, W. Zhang, Y. Zhang, and W. Zhou, “Empirical properties of inter-cancellation durations in the Chinese stock market,” vol. 2, no. March, pp. 1–12, 2014.

[10] A. D. Anastasiadis, M. P. de Albuquerque, M. P. de Albuquerque, and D. B. Mussi, “Tsallis q-exponential describes the distribution of scientific citations-a new characterization of the impact,” *Scientometrics*, vol. 83, no. 1, pp. 205–218, 2010.

[11] M. I. Bogachev, A. R. Kayumov, and A. Bunde, "Universal Internucleotide Statistics in Full Genomes: A Footprint of the DNA Structure and Packaging?," *PLoS One*, vol. 9, no. 12, p. e112534, 2014.
[12] C. Beck, "Generalized statistical mechanics of cosmic rays," *Phys. A Stat. Mech. its Appl.*, vol. 331, no. 1–2, pp. 173–181, Jan. 2004.
[13] F. Vallianatos, G. Michas, and G. Papadakis, "Non-extensive and natural time analysis of seismicity before the Mw6.4, October 12, 2013 earthquake in the South West segment of the Hellenic Arc," *Phys. A Stat. Mech. its Appl.*, vol. 414, pp. 163–173, Nov. 2014.
[14] a. Namaki, Z. Koohi Lai, G. R. Jafari, R. Raei, and R. Tehrani, "Comparing emerging and mature markets during times of crises: A non-extensive statistical approach," *Phys. A Stat. Mech. its Appl.*, vol. 392, no. 14, pp. 3039–3044, Jul. 2013.
[15] W. Li, Q. a. Wang, L. Nivanen, and a. Le Méhauté, "How to fit the degree distribution of the air network?," *Phys. A Stat. Mech. its Appl.*, vol. 368, no. 1, pp. 262–272, Aug. 2006.
[16] F. Vallianatos and D. Triantis, "A non-extensive view of the Pressure Stimulated Current relaxation during repeated abrupt uniaxial load-unload in rock samples," *EPL (Europhysics Lett.*, vol. 104, no. 6, p. 68002, 2013.
[17] C. Tsallis, *Introduction to nonextensive statistical mechanics: approaching a complex world*. New York: Springer, 2009.
[18] J. Laherrère and D. Sornette, "Stretched exponential distributions in Nature and Economy: ``Fat tails'' with characteristic scales," *Eur. Phys. J. B*, vol. 2, pp. 525–539, 1998.
[19] C. Tsallis, "Possible generalization of Boltzmann–Gibbs statistics," *J. Stat. Phys.*, vol. 52, pp. 479–487, 1988.
[20] Y. Goegebeur and A. Guillou, "Goodness-of-fit testing for Weibull-type behavior," *J. Stat. Plan. Inference*, vol. 140, no. 6, pp. 1417–1436, Jun. 2010.
[21] C. R. Shalizi, "Maximum Likelihood Estimation for q -Exponential (Tsallis) Distributions," 2007. [Online]. Available: arXiv:math/0701854v2 [math.ST].
[22] J.-F. Bercher and C. Vignat, "A new look at q-exponential distributions via excess statistics," *Phys. A Stat. Mech. its Appl.*, vol. 387, no. 22, pp. 5422–5432, Sep. 2008.
[23] J. A. Nelder and R. Mead, "A Simplex Method for Function Minimization," *Comput. J.*, vol. 7, no. (4), pp. 308–313, 1965.
[24] D. Bratton and J. Kennedy, "Defining a standard for particle swarm optimization," in *Proceedings of the IEEE Swarm Intelligence Symposium (SIS 2007)*, 2007.
[25] S.-W. Lin, K.-C. Ying, S.-C. Chen, and Z.-J. Lee, "Particle swarm optimization for parameter determination and feature selection of support vector machines," *Expert Syst. Appl.*, vol. 35, no. 4, pp. 1817–1824, 2008.
[26] S.-W. Fei, M.-J. Wang, Y.-B. Miao, J. Tu, and C. Liu, "Particle swarm optimization-based support vector machine for forecasting dissolved gases content in power transformer oil," *Energy Convers. Manag.*, vol. 50, no. 6, pp. 1604–1609, 2009.
[27] W.-C. Hong, "Chaotic particle swarm optimization algorithm in a support vector regression electric load forecasting model," *Energy Convers. Manag.*, vol. 50, no. 1, pp. 105–117, 2009.
[28] B. Samanta and C. Nataraj, "Use of particle swarm optimization for machinery fault detection," *Eng. Appl. Artif. Intell.*, vol. 22, pp. 308–316, 2009.
[29] I. D. Lins, M. das C. Moura, and E. L. Droguett, *Support vector machines and particle swarm optimization: applications to reliability prediction.* Saarbrücken, Germany: Lambert Academic Publishing, 2010.
[30] I. D. Lins, M. das C. Moura, E. Zio, and E. L. Droguett, "A particle swarm-optimized support vector machine for reliability prediction," *Qual. Reliab. Eng. Int.*, vol. 28, pp. 141–158, 2012.
[31] E. L. Droguett, I. D. Lins, M. C. Moura, E. Zio, and C. M. Jacinto, "Variable selection and uncertainty analysis of scale growth rate under pre-salt oil wells conditions using support vector regression," *Proc. Inst. Mech. Eng. Part O J. Risk Reliab.*, May 2014.

[32] I. D. Lins, M. das C. Moura, E. A. L. Droguett, C. M. Jacinto, and E. Zio, “Failure prediction of oil wells by support vector regression with variable selection, hyperparameter tuning and uncertainty analysis,” *Chem. Eng. Trans.*, vol. 33, pp. 817–822, 2013.

[33] P. R. A. Firmino, M. das C. Moura, A. P. Oliveira, I. D. Lins, and E. L. Droguett, “Política ótima de manutenção preventiva de sistemas reparáveis baseada em confiabilidade,” in *Proceedings of the XX Congresso Pan-Americano de Engenharia Naval, Transporte Marítimo e Engenharia Portuária*, 2007.

[34] M. Schwaab, E. C. Biscaia, Jr., J. L. Monteiro, and J. C. Pinto, “Nonlinear parameter estimation through particle swarm optimization,” *Chem. Eng. Sci.*, vol. 63, no. 6, pp. 1542–1552, 2008.

[35] F.-K. Wang and P.-R. Huang, “Implementing particle swarm optimization algorithm to estimate the mixture of two Weibull parameters with censored data,” *J. Stat. Comput. Simul.*, vol. 84, no. 9, pp. 1975–1989, 2014.

[36] J. Kennedy, R. Eberhart, and Y. Shi, *Swarm intelligence*. San Francisco, USA: Morgan Kaufmann, 2001.

[37] F. Taubert, F. Hartig, H. J. Dobner, and A. Huth, “On the Challenge of Fitting Tree Size Distributions in Ecology,” *PLoS One*, vol. 8, no. 2, 2013.

[38] X. Chen, M. Foy, M. Kimmel, and O. Y. Gorlova, “Modeling the Natural History and Detection of Lung Cancer Based on Smoking Behavior,” *PLoS One*, vol. 9, no. 4, p. e93430, 2014.

[39] H. C. Moore, P. Jacoby, A. B. Hogan, C. C. Blyth, and G. N. Mercer, “Modelling the seasonal epidemics of respiratory syncytial virus in young children,” *PLoS One*, vol. 9, no. 6, pp. 1–8, 2014.

[40] A. Rajan and T. Malakar, “Optimal reactive power dispatch using hybrid Nelder–Mead simplex based firefly algorithm,” *Int. J. Electr. Power Energy Syst.*, vol. 66, pp. 9–24, 2015.

[41] R.-A. Hooshmand, M. J. Morshed, and M. Parastegari, “Congestion management by determining optimal location of series FACTS devices using hybrid bacterial foraging and Nelder–Mead algorithm,” *Appl. Soft Comput.*, vol. 28, pp. 57–68, 2015.

[42] S. Abedi, F. Farhadi, and R. B. Boozarjomehry, “Integration of CFD and Nelder-Mead algorithm for optimization of MOCVD process in an atmospheric pressure vertical rotating disk reactor,” *Int. Commun. Heat Mass Transf.*, vol. 43, pp. 138–145, 2013.

[43] A. Maria, S. Gonçalves, A. Maria, and S. Gonçalves, “O Problema de Min-Max-Min com restrições pelo Método de Nelder-Mead,” UFRJ, 2013.

[44] Y. Furuya, “Specimen size effects on gigacycle fatigue properties of high-strength steel under ultrasonic fatigue testing,” *Scr. Mater.*, vol. 58, no. 11, pp. 1014–1017, 2008.

[45] O. H. Basquin, “The Exponential Law of Endurance Tests,” in *Proceedings of the American Society for Testing and Materials*, 1910, pp. 625–630.

[46] F. N. Nwobi and C. A. Ugomma, “A Comparison of Methods for the Estimation of Weibull Distribution Parameters,” *Metod. Zv. - Adv. Methodol. Stat.*, vol. 11, no. 1, pp. 65–78, 2014.

[47] G. C. Blain, “Revisiting the critical values of the Lilliefors test : towards the correct agrometeorological use of the Kolmogorov-Smirnov framework,” *Agrometeorogy*, vol. 73, no. 2, pp. 192–202, 2014.

[48] W. Stute, W. G. Manteiga, and M. P. Quindimil, “Bootstrap Based Goodness-Of-Fit-Tests,” *Metrika*, vol. 40, pp. 243–256, 1993.

[49] R. Castro, “Lectures 2 and 3 - Goodness-of-Fit (GoF) Tests,” pp. 1–18, 2013.